FILTERLESS NON-DISPERSIVE INFRA-RED GAS DETECTION: A PROOF OF CONCEPT

Andrea De Luca[1], Syed Z. Ali[2], Richard H. Hopper[2], Sophie Boual[2], Julian W. Gardner[3], and Florin Udrea[1,2]*

[1]Department of Electrical Engineering, University of Cambridge, Cambridge, UK
[2]Cambridge CMOS Sensors, member of AMS AG group, AUSTRIA
[3]School of Engineering, University of Warwick, Coventry, UK

ABSTRACT

For the first time, we demonstrate the detection of carbon dioxide (CO_2) using a non-dispersive infra-red (NDIR) technique that does not require an expensive CMOS-incompatible optical filter. This is achieved by employing a differential IR thermopile detector with micro-engineered (plasmonic) optical properties, fabricated in a commercially available standard CMOS MEMS process. The proof of concept demonstrated here represents a milestone in low-cost gas sensing spectroscopy, and has the potential to impact profoundly in the entire IR field; many consumer electronics applications (wearables, smartphones, tablets and portable medical devices) will become viable, leading to high volume commercial applications for plasmonic devices.

INTRODUCTION

NDIR spectroscopy [1] relies upon the principle that each molecule absorbs IR radiation at specific wavelengths, thus providing excellent selectivity, stability, and sensitivity. NDIR is a detection technique widely used in air quality monitoring, medicine and numerous industrial applications, including those in harsh environments. Among the gases with absorption fingerprints in the mid-IR region (2–14 μm), CO_2 is the most commonly targeted by NDIR gas sensors (CO_2 absorbs at 4.26 μm), given the absence of other reliable techniques for its detection. NDIR sensors typically comprise *(i)* an IR emitter to generate IR radiation, *(ii)* an IR detector to sense IR radiation, *(iii)* an optical filter to select the range of wavelengths characteristic of the target gas, and *(iv)* an optical light path to guide IR radiation from the emitter to the detector. Figure 1 schematically shows the structure and the working principle of a NDIR sensor. The relatively high complexity, large size (order of cm^3) and high price of such sensors has so far hindered their use in consumer electronic applications (*e.g.* wearables, smartphones and tablets) requiring stringent specifications in terms of miniaturisation (size in the order of mm^3), costs (possibly below $1) and power consumption (in the order of microwatts). Exploiting standard CMOS processes is an attractive route toward the fabrication of low cost miniaturized IR emitters and detectors for such application. Traditional NDIR sensors employ broadband thermal emitters and broadband thermal detectors, and rely upon optical band-pass filters to achieve gas selectivity; this results in fixed spectral performance, additional costs (up to 2/3 of the total IR detector costs), large form factor and limited operating temperature range. The filters also add complexity in package manufacturing/assembly and system design, especially when high temperatures are involved. There have been several reports in literature, *e.g.* [2], suggesting that the emissivity/absorptivity of devices can be varied at particular wavelengths by using plasmonic structures, which are periodic structures created on a surface. However, the literature does not cover the idea of an array of detectors (with different tailored optical properties), nor cover any differential (or other) processing method to analyze the response of the detectors for the ultimate aim of filterless NDIR detection.

Our group has already shown in the past that plasmonic/metamaterial concepts can be successfully applied to CMOS IR devices [3], both emitters [4] and detectors [5], to tailor the emissive/absorptive optical properties of such devices. In absence of this optical micro-engineering approach, CMOS IR devices have shown poor/non-optimal spectral performance exclusively defined by the materials forming the devices [6-8].

In this paper we demonstrate CO_2 detection with a filterless NDIR sensor, wherein selectivity is achieved by employing a spectrally-selective CMOS MEMS IR detector based on a plasmonic dual thermopile differential approach.

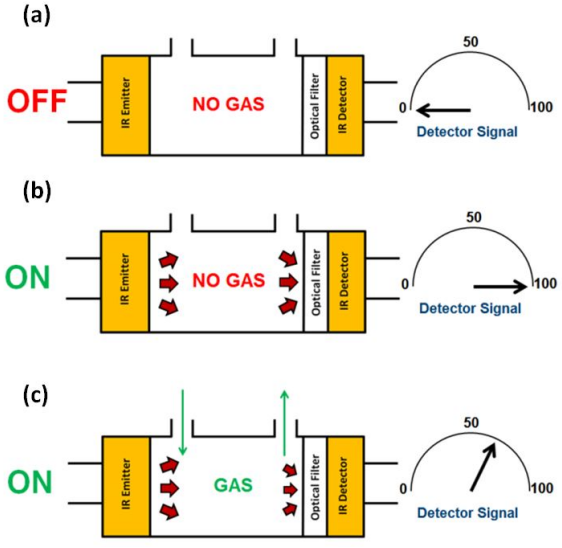

Figure 1 Schematic depiction of NDIR sensor working principle. (a) When the IR emitter is OFF, the signal on the IR detector is minimum. (b) When the IR emitter is ON and there is no gas in the cavity, the signal on the IR detector is maximum. (c) When the target gas is in the cavity, the signal on the IR detector decreases depending on the gas concentration following the Beer-Lambert law.

EXPERIMENTAL METHODS

The IR detector presented in this study was fabricated within a commercial foundry on 6" silicon-on-insulator (SOI) CMOS wafers, subsequently back-etched in the same foundry. It is important to highlight that the use of SOI does not restrict the ideas presented in this work, which can be extended to a bulk CMOS process as well as to processes employing substrates different from silicon. Of course the use of silicon guarantees a number of benefits including, among others, high volume production at low costs, high reproducibility from device-to-device/batch-to-batch/lot-to-lot and possibility to have electronics monolithically integrated on chip. In Fig. 2, a top view and schematic cross-section of the differential IR detector chip are presented. The chip comprises two separate IR thermal detectors: *(i)* a standard detector (Fig. 1a top left) and *(ii)* a plasmonic detector (Fig. 1a bottom right). Both detectors feature a thermopile embedded within a 750 µm side dielectric membrane released *via* deep reactive ion etching (DRIE). DRIE ensures maximum flexibility in the choice of the membrane shape, which was chosen to be square with rounded corners in order to improve the membrane's mechanical robustness (in comparison to a square membrane) and the IR sensing area (in comparison to a circular membrane). DRIE also allows near-vertical membrane cavity side-walls for enhanced detector packing density. Each thermopile is formed by 40 single crystal silicon n+/p+ thermocouples, joint together through ohmic aluminum contacts in order to avoid formation of rectifying junctions. Each thermocouple has its cold junction on the substrate and its hot junction on the membrane. The plasmonic detector is characterized by an additional patterned metal layer (plasmonic layer) within the membrane above the thermopile. This layer is introduced to engineer the absorption properties of the plasmonic detector, *via* excitation of specific and tailorable surface plasmon resonances [9]. In this specific chip, the plasmonic layer is composed of aluminum cylinders arranged in a hexagonal symmetry. The spacing between two neighboring cylinders is 2.6 µm, and the radius of each cylinder is 0.8 µm. The plasmonic structures were chosen to be fully embedded within the dielectric layers in order to avoid direct exposure of the metal to the environment and possible fouling effects, which would be detrimental for the long term stability of the spectral performance of the device. Diode temperature sensors were also co-integrated on the chip for ambient/case/package temperature monitoring and thus possible implementation of thermopile cold junction compensation schemes.

As fabricated devices were then laser diced in a commercial dicing-house and wedge bonded in-house onto TO39 packages.

The spectral performance of each detector (of an unpackaged chip) was characterized in the 3-15 µm wavelength range using a Fast Fourier Transform Infra-Red (FTIR) method, conducted with a Scimitar FTIR System, in both reflection (*R*) and transmission (*T*) mode. A standard gold plate was used for calibration of the reflection measurements, and a KBr disk was used for the transmission measurements. A 15× objective lens was used with a numerical aperture of 0.5. Absorptivity (*A*) for each detector was calculated as *A=1-R-T*. In Fig. 3 and Fig. 4 FTIR spectra for the standard and the plasmonic detector are reported, respectively. In Fig. 5 the calculated differential absorptivity spectrum ($A_{differential} = A_{plasmonic} - A_{standard}$) is presented along with the plasmonic detector absorptivity spectrum ($A_{plasmonic}$) and the standard detector absorptivity spectrum ($A_{standard}$).

Filterless NDIR CO_2 detection is shown in Fig. 6. A prototype capnometer (schematically depicted as inset of Fig. 6) was used to demonstrate the effectiveness of employing plasmonic structures to provide our differential IR detector with spectral filtering capabilities. A proprietary plasmonic IR emitter was used as a light source in the experiments. Packages featuring metallic reflectors were also employed to improve IR light collimation from the source to the detector. A differential amplifier (gain of 1,000) was implemented on a PCB to obtain the IR detector differential signal.

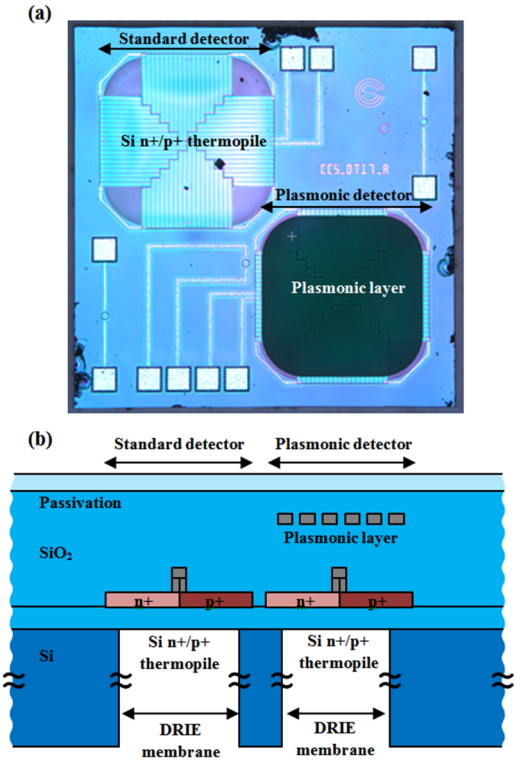

Figure 2: (a) Differential IR detector chip (size: 1.6mm×1.6mm); (b) Schematic depiction (not to scale) of the differential IR detector chip cross-section. Note the plasmonic layer absorbs most of the light generated by the microscope, thus looking black and "shadowing" the thermopile underneath.

RESULTS AND DISCUSSION

In Fig. 3, the optical properties of the standard detector are presented. The absorptivity ($A_{standard}$) below 8 µm is strongly suppressed. Around 4.26 µm (CO_2 absorption region) roughly 40% of the incoming radiation is reflected and 45% is transmitted by and through the membrane, resulting in low (15%) absorptivity. In Fig. 4, the optical properties of the plasmonic detector are presented. Clearly, the absorptivity ($A_{plasmonic}$) below 8 µm

is enhanced, in comparison to the standard detector; around 4.26 μm its absorptivity almost reaches 80%. This is due to plasmonic resonance effects, resulting in a localized increase in electric field (around the plasmonic structures) and consequent enhancement of light/matter interaction phenomena, which in turn cause an increase in the membrane temperature (in comparison to the standard detector), transduced in a higher electric signal by the thermopile. However, a large proportion of this electrical signal is still due to IR radiation outside the range of interest, and thus not useful for CO_2 detection. More interestingly, in Fig. 5, the differential spectrum ($A_{differential}$) features suppressed absorptivity (<30%) above 5 μm and high absorptivity (~65%) around 4.26 μm. In this case, a bigger portion of the differential IR detector output signal is proportional to IR radiation in the wavelength range of interest for CO_2 detection. We have thus shown that with our differential approach it is possible to embed enhanced spectral filtering features at the device level compatible to the CO_2 absorption region. This results in the possibility to build an NDIR sensor that does not require a large expensive optical filter. The experimental proof of concept is shown in Fig. 6, where the CO_2 detection capabilities of a prototype filterless NDIR sensor employing our differential IR detector are presented. The differential IR detector output (*i.e.* the difference between the output of the thermopile within the plasmonic detector and the output of the thermopile within the standard detector) is shown as a function of time in dry air for different pulses of CO_2. Absorption of IR radiation by the CO_2 molecules results in a decrease in the detector signal. The higher the number of molecules (*i.e.* CO_2 concentration), the higher the absorption within the gas cell and thus the lower the differential detector signal. In Fig. 7, the differential IR detector output change is plotted as a function of CO_2 concentration for tests carried out at three different relative humidity (RH) levels (namely dry air, 40% RH and 80% RH). Linear interpolations of the obtained data are superimposed to show that the effect of humidity is minimal. This is due to the fact that $A_{differential}$ in the H_2O absorption range is suppressed down to less than 30%. Specificity against CO (2000ppm) was also achieved.

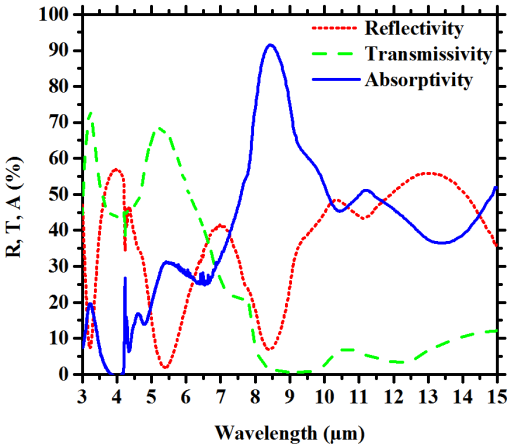

Figure 3: FTIR-measured reflectivity (R), transmissivity (T), and calculated absorptivity (A=1-R-T) of the standard detector.

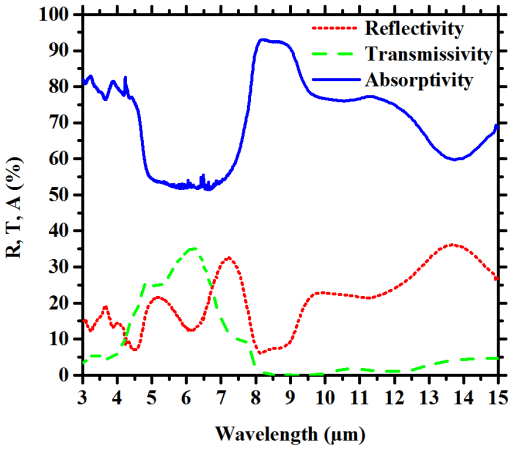

Figure 4: FTIR-measured reflectivity (R), transmissivity (T), and calculated absorptivity (A=1-R-T) of the plasmonic detector.

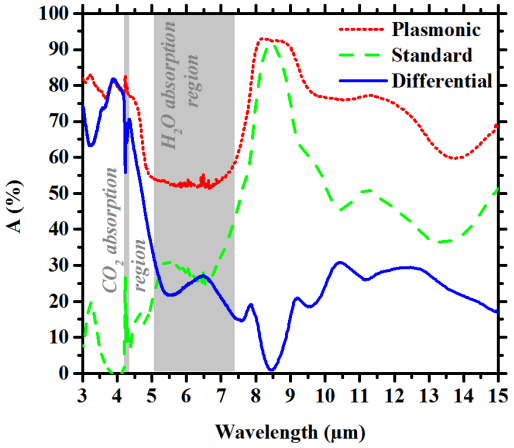

Figure 5: Absorptivity spectra for plasmonic detector ($A_{plasmonic}$, from Fig. 4), standard detector ($A_{standard}$, from Fig. 3), and resulting spectrum ($A_{differential} = A_{plasmonic} - A_{standard}$) for the differential IR detector. Absorption regions for carbon dioxide and water molecules are also shown.

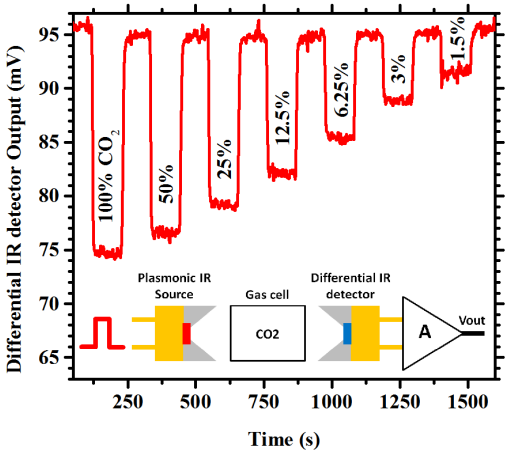

Figure 6: Filterless NDIR sensor output as a function of time for different CO_2 pulses in dry air. Inset: schematic depiction of the filterless NDIR sensor.

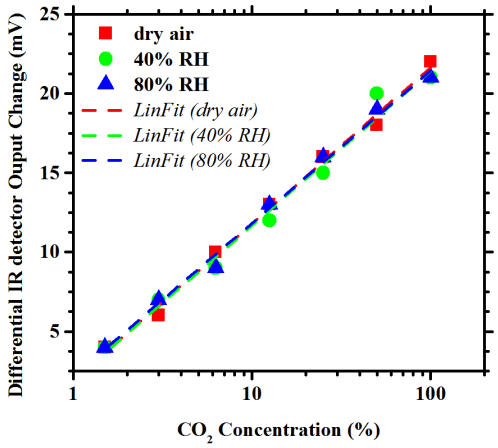

Figure 7: Filterless NDIR sensor output change as a function of CO_2 concentration for different levels of relative humidity (dry air, 40%RH and 80%RH).

CONCLUSION

In this paper, we have demonstrated a plasmonic filterless NDIR gas detection. Carbon dioxide was chosen as the target gas, due to the huge market request for low cost, miniature, sensitive and reliable CO_2 gas sensors (CO_2 sensors account for more than 25% of the global gas sensor market, estimated to be worth around $2.5B by 2020). Filterless detection was achieved by engineering the optical properties of a thermopile based CMOS IR detector. More specifically, surface plasmon resonances were exploited to embed at device level spectral filtering capabilities, allowing the NDIR sensor to be selective towards CO_2 without the need for a discrete optical filter.

FTIR measurements were carried out to verify the effect of the introduction of a plasmonic layer within a typical thermopile IR detector, and significant improvement of the absorption properties of the detector around 4.26 µm was proven. Furthermore, it was shown that the differential approach results in strongly reduced absorption in the spectral range not of interest for CO_2 detection, where other interfering gases (*e.g.* H_2O between 5 µm and 7.5 µm, and CO between 4.5 µm and 5 µm) have their absorption fingerprints.

The effectiveness of this approach was experimentally proven with a prototype capnometer-type filterless NDIR sensor employing our differential IR detector. A clear response to CO_2 (1.5 to 100% range, limited by our gas delivery system) was obtained as well as selectivity against humidity (up to 80%, limited by our gas delivery system) and CO (up to 2000 ppm, limited by our gas delivery system).

To conclude, we strongly believe our pioneering work on CMOS IR emitters and detectors with engineered spectral properties will lead to a new generation of IR devices for low cost, ultra-miniaturised IR sensing applications.

ACKNOWLEDGEMENTS

This work was partly supported through the EU FP7 project MSP (611887).

REFERENCES

[1] J. Hodgkinson, R. Smith, W. O. Ho, J. R. Saffell, and R. P. Tatam, "Non-dispersive infra-red (NDIR) measurement of carbon dioxide at 4.2 µm in a compact and optically efficient sensor," *Sensors and Actuators B: Chemical,* vol. 186, pp. 580-588, 2013.

[2] V. Shklover, L. Braginsky, G. Witz, M. Mishrikey, and C. Hafner, "High-temperature photonic structures. Thermal barrier coatings, infrared sources and other applications," *Journal of Computational and Theoretical Nanoscience,* vol. 5, pp. 862-893, 2008.

[3] S. Z. Ali, F. Udrea, J. Gardner, R. H. Hooper, A. De Luca, M. F. Chowdhury, and I. Poenaru, "Plasmonic IR devices," US9214604, 2015.

[4] A. Pusch, A. De Luca, S. S. Oh, S. Wuestner, T. Roschuk, Y. Chen, S. Boual, Z. Ali, C. C. Phillips, and M. Hong, "A highly efficient CMOS nanoplasmonic crystal enhanced slow-wave thermal emitter improves infrared gas-sensing devices," *Scientific reports,* vol. 5, 2015.

[5] M. Chowdhury, S. Ali, S. Boual, R. Hopper, and F. Udrea, "Development of plasmonic MEMS CMOS infrared sensors for occupancy detection," in *Solid-State Device Research Conference (ESSDERC), 2016 46th European*, 2016, pp. 97-100.

[6] A. De Luca, M. Cole, A. Fasoli, S. Ali, F. Udrea, and W. Milne, "Enhanced infra-red emission from sub-millimeter microelectromechanical systems micro hotplates via inkjet deposited carbon nanoparticles and fullerenes," *Journal of Applied Physics,* vol. 113, p. 214907, 2013.

[7] R. Hopper, S. Ali, M. Chowdhury, S. Boual, A. De Luca, J. W. Gardner, and F. Udrea, "A CMOS-MEMS thermopile with an integrated temperature sensing diode for mid-IR thermometry," *Procedia Engineering,* vol. 87, pp. 1127-1130, 2014.

[8] A. De Luca, M. Cole, R. Hopper, S. Boual, J. Warner, A. Robertson, S. Ali, F. Udrea, J.W. Gardner, and W. Milne, "Enhanced spectroscopic gas sensors using in-situ grown carbon nanotubes," *Applied Physics Letters,* vol. 106, p. 194101, 2015.

[9] S. A. Maier, *Plasmonics: fundamentals and applications*: Springer Science & Business Media, 2007.

CONTACT

*A. De Luca; tel. +44(0)1223748311; ad597@cam.ac.uk